Journal of Materials Science & Surface Engineering Vol. 5 (1), 2017, pp 504-508

Contents lists available at http://www.jmsse.org/

Journal of Materials Science & Surface Engineering

Picosecond Laser Cleaning of Hot Stamped 22MnB5 Steel

Hamza Messaoudi*, Salar Mehrafsun, Waldemar Tromenschläger

BIAS - Bremer Institut für angewandte Strahltechnik, Klagenfurter Str. 5, 28359 Bremen, Germany.

Article history

Received: 24-Dec-2016
Revised: 06-Jan-2017
Available online: 23-Jan-2017

Keywords:
Ultrashort pulsed lasers,
Laser micro machining,
Surface modification,
Stamping,
Weld preparation

Abstract

Increased lightweight design in automotive industries is followed by increased production of high strength steel components. During the hot stamping procedure, an Al-Si coating is applied to the surface of these steels as a preventive measure against oxidation. For subsequent welding applications, this coating caused a weakening of the mechanical properties such as tensile strength and hardness. In this work, an ultra-short pulsed laser removal of the Al-Si coating as a weld preparation technique was investigated. The influence of wavelength as well as pulse energy and scanning parameters on the removal depth and rate are discussed. Furthermore, the large-area picosecond laser removal of the Al-Si coating was analyzed under consideration of removal quality and processing efficiency.

Introduction

The reduction of CO_2 emissions and fuel consumption represent the overriding aims in the automotive industry. For their fulfillment, different strategies, such as the development of hybrid and electric-car technology, the efficiency increase of diesel and gasoline engines and the lightweight design are followed in parallel over the last decades [1]. By 2030, the use of lightweight materials in automotive production is expected to make up about 70% of all materials [2]. Thereby, (ultra) high-strength steels (UHSS) are estimated to be the principal material in car chassis for reasons of safety and crashworthiness with a percentage of 38% in 2030. Due to tensile strengths, greater than 1500 MPa, parts made of UHSS are predestined as crash relevant structural components in body shells like the B-pillar reinforcement to the roof panel or the tunnel [3].

Because of increased fabrication process efficiency, hot stamping has been established in series production chains to manufacture UHSS parts [4]. A blank of hardened boron steel such as 22MnB5 is heated up in a furnace, transferred to the press and subsequently formed and quenched. This is called the direct hot stamping [5]. Otherwise the indirect hot stamping is characterized by an indirect cold performing of the blank followed by an austhenitization and quenching to the final shape. In order to avoid surface oxidation and decarburization, occurring because of steel-air contact, 22MnB5-blanks are pre-coated by protective Al-Si layer [5].

Investigations on subsequent welding applications of hot-stamped parts, such as laser beam [6] and GMA welding [7], have determined a strong formation of Fe-Al intermetallic phase caused by the dilution of the Al-Si layer into the weld pool. This brittle phase spreads along the fusion line and leads to decreased material ductility as well as its tensile strength and elongation. Comparative studies on the laser welding of hot stamped parts with and without Al-Si coating, as carried out in [8] and [9], have shown that the best tensile strength and elongation were obtained at workpieces where the Al-Si-coating has been removed. These corresponds to 1450 MPa and 3% tensile strength and elongation, respectively. In addition, the removal of Al-Si layer leads to complete transformation to martensite and avoids the formation of ferrite in the weld zone. Thereby, the Vickers hardness is constantly higher than the base material with values between 450 HV and 550 HV. This indicates that removal of Al-Si coating as a weld preparation for welding applications of hot stamped steels is required and beneficial.

Within this work, an ultra-short pulsed laser removal of the Al-Si coating of hot stamped 22MnB5-blanks will be investigated. The influence of wavelength as well as pulse energy and scanning parameters on the removal depth and rate will be discussed. Furthermore, the large-area picosecond laser removal of the Al-Si coating will be analyzed under consideration of processing efficiency and removal quality.

Experimental

Press-hardened boron steel *22MnB5 AS140* from ThyssenKrupp was used. This steel has a chemical composition (max. mass%) of 0.25 C-0.40 Si-0.025 P-0.010 S-1.4 Mn-0.015 Al-0.5 (Cr+Mo)-0.05 Ti-0.005 B and a thickness of 2 mm. It is delivered entirely coated with an Al-Si alloy (0.9 Al + 0.1 Si) and a concentration of 140 g/m^2. The coating is applied using a hot dipping procedure, in which the layer thickness is determined by air spraying using nozzles under defined angles.

To remove the Al-Si layer – as a preparation for following welding applications – a picosecond laser system (TruMicro5050 from Trumpf GmbH) was used. It operates at a wavelength of 1030 nm in its fundamental Gaussian mode and delivers an average maximum power of 50 W at 200 kHz. It produces pulse widths of < 10 ps and maximum pulse energy of 250 µJ. The collimated laser beam is first expanded and then coupled into a

Corresponding author. Tel +49 421 218 58045; Fax: +49 421 218 58063
E-mail address: messaoudi@bias.de

frequency conversion system (Xiton box from Xiton), which allows the second harmonic generation (wavelength of 515 nm) in a separated optical path. Thereby, the maximum average power is about 33 W and the maximum pulse energy is 150 µJ. Depending on the used wavelength the collimated beam is coupled into one of two programmable galvanometer scanners (HurriScan 14 from ScanLab), which enable process speeds up to 12 m/s. The orthogonal arrangement of the scanner mirrors directs the beam down towards the workpiece using an F-Theta lens (160 mm focal length). This enables both a large scan fields (100 mm x 100 mm) and a small focused laser spot sizes (48 µm and 24 µm, for 1030 nm and 515 nm, respectively) at perpendicular incidence of the laser beam. To adjust the focal plane, the workpiece is mounted on a z-axis.

Throughout this work, different parameters were varied, with the aim to determine their influences. These are illustrated in Table 1. Thereby, pulse duration t_p, pulse repetition rate f_{Rep} and the focal position Δz were kept constant at 6 ps, 200 kHz and 0 mm, respectively.

Table 1: Varied parameters of ps-laser ablation

Parameters	Unit	at 1030 nm	at 515 nm
Pulse energy E_p	µJ	5 … 30	3 … 40
Number of pulses N_p	-	1 … 1000	1 … 1000
Number of scans N_s	-	1 … 500	1 … 500
Scan speed v_{scan}	mm/s	100 … 10000	1 … 4000

The investigations were carried out for single spots, line scans as well for large areas with the aim to determine the wavelength-dependent removal quality and efficiency. The resulting width, depth and topography of ps-laser ablated parts were evaluated using different methods:

- Laser confocal microscopy to analyze the surface quality and to obtain 3D-profiles.
- Cross-section analysis – as destructive testing method –to determine the ablation geometries (width and depth) as well as the ablation homogeneities.
- Energy dispersive spectroscopy (EDS) for element analysis at the ablated surfaces.

Results

Characterization of the Al-Si coating

The topographical analysis of the Al-Si coating surface, as illustrated in Fig. 1, shows an inhomogeneous distribution of the coating at the surface as well as in the depth.

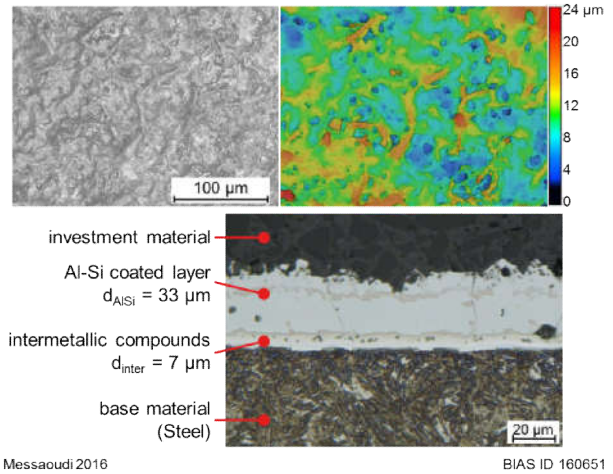

Figure 1: 3D-Surface topography profiles of the Al-Si coating (above) and cross-section of the hot stamped steel (below)

Following the DIN EN ISO 4287 the calculated arithmetic mean roughness R_a and the maximum height R_z were found to be 2.5 µm ± 0.35 µm and 28 µm ± 6.8 µm, respectively. The cross-section (Fig. 1-below) shows the microstructure of the hot stamped 22MnB5 steel. The measured average thickness of the Al-Si layer (d_{AlSi}) amounts 33 µm ± 8 µm. Besides the coating non-homogeneity, pores and micro-cracks could be observed. Between Al-Si layer and base material a 7 µm thick intermetallic compound is located. It consists of $FeAl_3$ and Fe_2Al_5 and has the function of enhancing the hardness. These AlSi-phases are formed during the austenitization (under temperatures greater than 650 °C) due to diffusion processes that occur at the interface between the base steel material and the coating. They lead not only to a hardness increase [10] but also to a higher crack initiation and propagation [11].

Ablation behavior at λ = 1030 nm

To characterize the interaction between ps-Laser pulses and Al-Si surface, the workpiece was first irradiated under a fixed exposure, where only pulse energy E_p and number of pulses N_p were varied. As a result of the interaction, measured spot diameters (mostly observed after $N_p > 2$ pulses) between 39 µm and 55 µm have been measured, which increase linearly with the number of pulses N_p. However, a notable material removal has been observed first for $N_p > 100$ pulses with values between $0.5 \cdot 10^{-5}$ mm³ and $3 \cdot 10^{-5}$ mm³, as illustrated in Fig. 2. Thereby, it

$_p$ and E_p are, the more material can be removed.

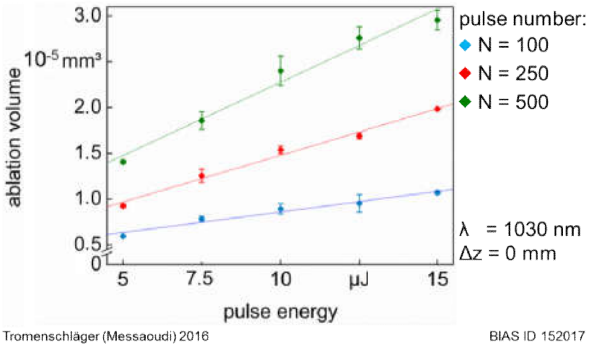

Figure 2: Removal volume at single ablation spots in dependence of the pulse energy E_p at 100, 250 and 500 pulses

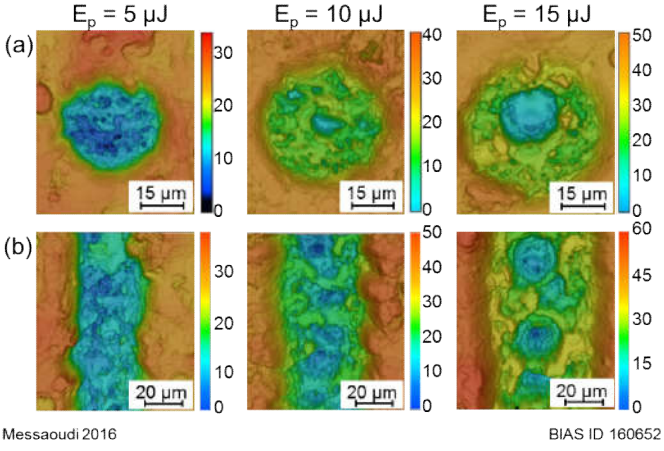

Figure 3: 3D-Profiles of ablated surfaces in dependence of E_p after laser irradiation at fixed exposure with N_p = 500 pulses (a) and at scanning mode of single lines with v_{scan} = 1 m/s and N_s = 100 (b)

The surface characterization of ablated spots shows the thermal impact as the result of increased pulse energy (see Fig. 3.a). Due to coating non-homogeneities, the roughness of the Al-Si surface caused an inhomogeneous absorption of laser light, which results in a non-uniform material removal. This effect becomes stronger at higher laser energy input. At $E_p = 5$ µJ, the maximum height R_z on the ablation plane does not exceed 15 µm, while R_z does not fall below 25 µm at $E_p > 10$ µJ and reaches values larger than 45 µm at 15 µJ. Here the central parts of the removal spot are preferably stronger ablated than outer parts due to the Gaussian intensity distribution at the surface. The same is observed during the scanning of single lines. Fig. 3.b shows exemplary the removal lines after 100 scans at scan speed of 1 m/s. The higher the pulse energy is, the broader and more inhomogeneous is the material removal.

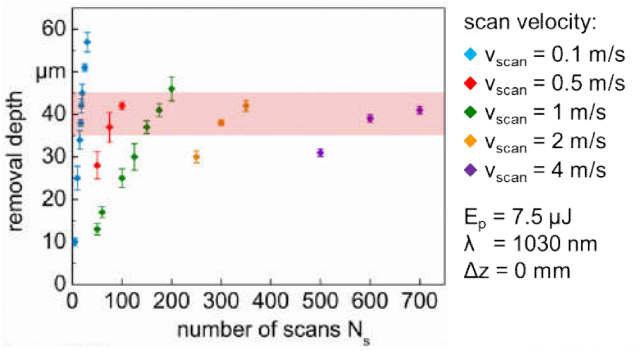

Figure 4: The removal depth in dependence of scan velocity v_{scan} and number of scans N_s at $E_p = 7.5$ µJ; The red bar indicates the typical thickness of the Al-Si layer (cf. fig. 1) to be ablated

Figure 4 shows exemplarily the influence of number of scans N_s and scan velocity v_{scan} on the resulting removal depth at a constant pulse energy $E_p = 7.5$ µJ. To remove the Al-Si layer (indicated by the light red bar), as shown in Fig. 4, the number of scans N_s increases with the scan velocity from 17 scans, 170 scans to 670 scans at v_{scan} of 0.1 m/s, 1 m/s and 4 m/s, respectively. For a processing distance of e.g. 1 mm, a constant machining time of 170 ms ± 5 ms can be ascertained.

When additionally, considering the total input energy, which can be defined as the accumulated energy per unit length S_E:

$$S_E = N_S \cdot \frac{E_p \cdot f_{rep}}{v_{scan}} \left[\frac{\text{mJ}}{\text{mm}}\right], \qquad (1)$$

it becomes apparent that the total input energy needed to remove the coating layer is mainly dependent on the pulse energy. At $E_p = 7.5$ µJ, a minimum S_E-value of 255.75 ± 7.65 mJ/mm is required independent on the applied scan velocity and scan repetitions.

In Fig. 5, the removal depth is illustrated in dependence of accumulated energy per unit length S_E and the pulse energy E_p. It has to be noticed that each determined S_E value pertains to specific pulse energy and was obtained from several combinations of scan velocities v_{scan} and number of scan N_s. For the ablation of the Al-Si layer and the underlying intermetallic compounds minimum S_E values ranging between 200 mJ/mm and 380 mJ/mm at pulse energies from 5 µJ to 15 µJ are required. It can therefore be stated that the higher the pulse energy is the more energy input per unit length is needed.

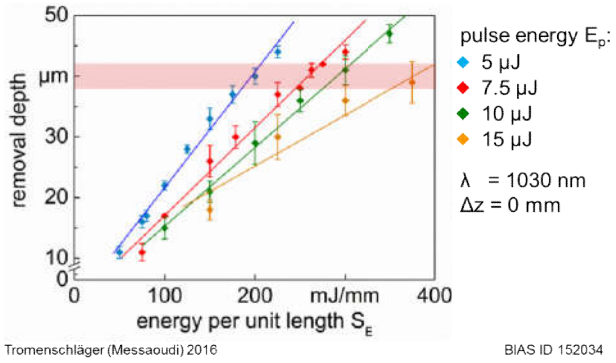

Figure 5: Measured removal depths at λ = 1030 nm as function of energy per unit length S_E for different pulse energies E_p; the light red bar assigns a removal depth around 40 µm

Ablation behavior at λ = 515 nm

Due to equal focal lengths of 160 mm of the used f-theta lenses, the focus spot size of the generated second harmonic (515 nm) is 24 µm, which is half of that of the fundamental wavelength. Knowing that the maximum pulse energy is 150 µJ, the maximum intensity at the Al-Si surface is about 26.5 MW/cm² (10 times higher than the intensities at λ = 1030 nm). Nevertheless, a surface modification was detected first at pulse energies $E_p > 9$ µJ and at pulse numbers $N_p > 100$.

The ablated spots ranged between 20 µm and 60 µm in diameter. To ensure a degree of pulse overlap greater than 60%, the scan speed for the removal at λ = 515 nm was limited to 2 m/s. As observed with the fundamental wavelength, the pulse energy strongly influences the geometry of the removed lines; both depth and width increase with rising pulse energies.

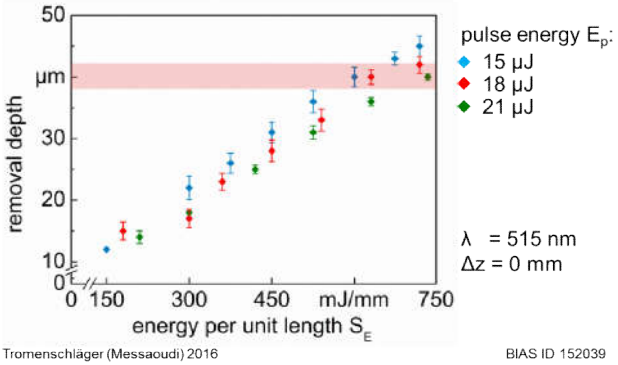

Figure 6: Measured removal depths at λ = 515 nm as function of energy per unit length SE for different pulse energies E_p

Despite the smaller spot size in focus plane, the used pulse energies necessary for the material ablation at 515 nm were found to be almost 2 times higher than those at 1030 nm. This effect is reflected also on the required energies per unit length. For the ablation of the 40 µm-layer an S_E of about 600 mJ/mm is necessary at pulse energy of 15 µJ; whereas at $E_p = 21$ µJ about 720 mJ/mm are needed (see Fig. 6).

Large area material removal

For an efficient large area removal of the Al-Si layer and the underlying intermetallic compounds, the lateral overlap between two scan lines should be identified. For that, the hatching distance between single scan lines has been varied between 5 µm and 20 µm. As can be seen in Fig. 7, a lateral overlap d_y of 10 µm (for both wavelengths 1030 nm and 515 nm) was found to be suitable for a smooth removal. Apart from that, the removal was found to

be non-uniform due to insufficient overlap ($d_y > 10$ µm) or heat accumulation effects ($d_y < 10$ µm).

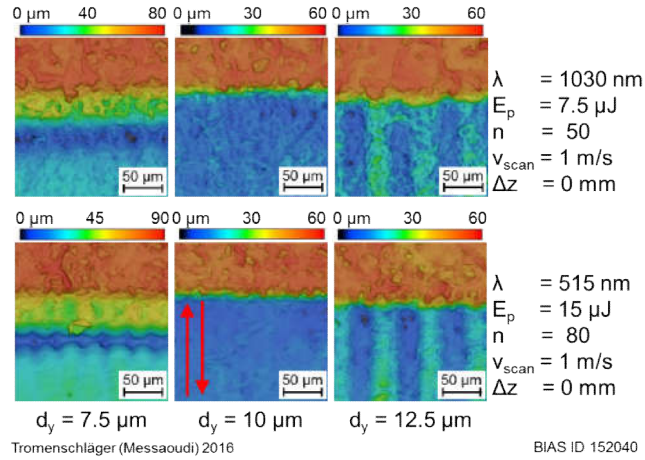

Figure 7: Influence of lateral overlap d_y on the homogeneity of large-area removal at λ = 1030 nm (above) and at λ = 515 nm (below); the red arrows indicate the scan direction

As mentioned before, the Al-Si layer can be entirely removed at required energies per unit length depending on the pulse energy. This can be realized using either slow scan speeds and low number of scans or fast scan speeds and high number of scans. In the following the scan speed was kept constant at v_{scan} = 1 m/s. As can be seen in Fig. 8, 45 scans to 80 scans are required at λ = 515 nm, whereas 40 scans to 70 scans are necessary at λ = 1030 nm.

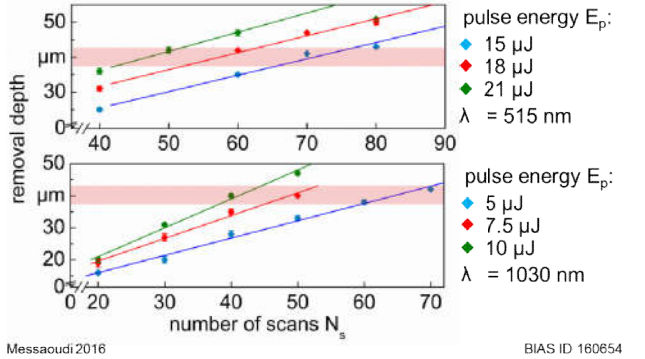

Figure 8: Removal depth as function of the number of scan N_s at v_{scan} = 1 m/s and different pulse energies and for 515 nm (above) and 1030 nm (below)

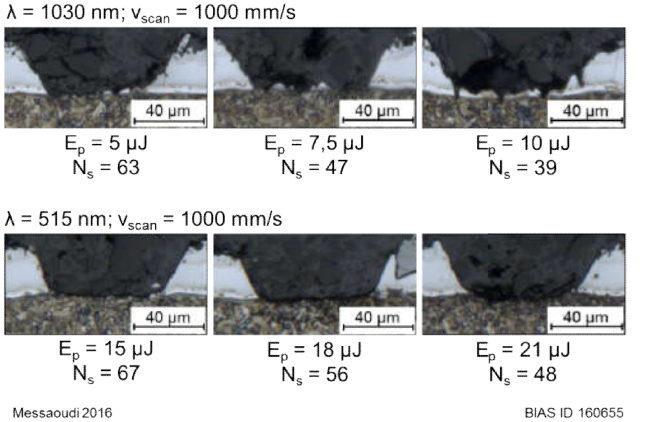

Figure 9: Cross sections of 100 µm wide processed areas with E_p-N_s combinations required for the ablation of 40 µm at v_{scan} = 1 m/s, λ = 1030 nm (above) and λ = 515 nm (below)

The resulting cross sections of ablated areas of 100 µm width are illustrated in Fig. 9. The number of scans N_s was determined from the associated red colored bar in Fig. 8, which corresponds to a removal depth of 40 µm. At λ = 1030 nm, the processed areas appeared to be inhomogeneous (residues in the bottom of the removed areas). This non-removed part becomes larger with increased pulse energy. The same has been observed with single line ablation (Fig. 3) and can be traced back to a locally inhomogeneous absorption of laser light caused by the non-uniform element distribution of the Al-Si coating. In contrast, the ps-laser removal at λ = 515 nm is more homogeneous and shows no residues. Thereby the flank angles achieved at both wavelengths are ranging between 75 ° and 78 °.

Discussion

In this work, the feasibility of ps-laser cleaning in removing the Al-Si coating and the underlying intermetallic compounds from hot-stamped 22MnB5-steel is successfully demonstrated. Thereby, the minimum energy per unit length S_E as well as the processing time required for the removal of the defined 40 µm thick layer are primary dependent on the pulse energy E_p and can be set with different combinations of scan velocity v_{scan} and scan repetitions N_s, as illustrated in Fig. 5 and Fig. 6. Here, it is recommended to use high scan velocities, if the pulse overlap degree is greater than 60% to realize a continuous removal over the scan path. The removal quality can be then better predicted due to the low ablation rates per scan and the avoidance of heat accumulation effects, which can lead to broad removal grooves and increased liability for non-homogeneities (see Fig. 3).

Despite slightly higher absorption coefficient of aluminum (as the dominating coating material) and higher intensities at the focal position at λ = 515 nm (due to smaller spot size), the pulse energies E_p required for the coating removal were found to be at least twice higher compared to those needed at 1030 nm. This effect has been also observed during the ablation of aluminum in noble gases [12] and liquid environments [13] and was attributed to the higher thermal impact at longer wavelengths. Similar is reflected in the determined input energies per unit lengths S_E. Regarding the pulse energy, S_E-values between 200 mJ/mm and 400 mJ/mm were required for the removal of the 40 µm thick layers at 1030 nm. In contrast, at 515 nm the S_E-values were ranging between 600 mJ/mm and 750 mJ/mm. Regarding the removal quality, it has been observed that the ablation at 515 nm is smoother and more homogeneous. This can be explained by the lower ablation rates at the visible wavelength. Moreover, occurred non-uniform removal can be traced back to the Gaussian intensity profile of the laser beam as well as to the inhomogeneous element distribution and surface decontaminations [14].

To identify the surface integrity after the ps-laser ablation, EDS-analysis was carried out. Fig. 10 shows the SEM-images (scanning electron microscopy) of the initial Al-Si surface as well as the processed surfaces at both wavelengths. At 1030 nm, the used parameter combination appeared to result a bump formation on the surface of the base metal. According to [15], this is caused by heat accumulation during processing. At 1030 nm, an inhomogeneous absorption enhances this effect due to local multi-reflections. In contrast, the surface processed at 515 nm is smoother and does not have any significant bump formation. In general, the arithmetic mean roughness R_a and the maximum height R_z have been reduced down to values of 1.45 µm and 11.5 µm, respectively. Furthermore, a comparison of the mass weight of the elements Fe, Al and Si on the initial and processed surfaces indicates clearly a strong reduction of Al and Si due to the cleaning process. Nevertheless, a residual amount of about 5% Al and 1% Si has been also detected, which can be explained by a locally-

incomplete removal or by a diffusion of Al and Si into the surface of the base metal.

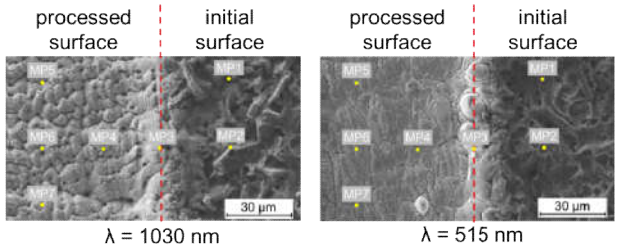

element	initial surface	processed at 1030 nm	processed at 515 nm
Fe	42,62 ± 6,2	88,6 ± 5,52	86,15 ± 11,06
Al	36,25 ± 5,62	3,48 ± 1,96	6,31 ± 2,84
Si	4,6 ± 1,8	0,94 ± 0,39	1,26 ± 0,73

Messaoudi 2016 BIAS ID 160656

Figure 10: SEM-pictures showing the transition from initial and ps-laser processed surfaces at 1030 nm and 515 nm (above); marked points indicate the measurement points used for an EDS-analysis (below)

Regarding the process efficiency, it was found that the scan repetitions N_s and thereby also the processing time could be significantly reduced down to 66% for large-area ablation compared to the single lines. This is caused by the lateral overlap of d_y = 10 µm, which resultsin hatching degrees of 58% and 79%, at 515 nm and 1030 nm, respectively. Furthermore, ablation rates of up to 16 mm²/min could be achieved during the removal of the 40 µm thick layer (Al-Si layer and the underlying intermetallic compounds) depending on the used parameters. In addition, it was ascertained that higher pulse energies can increase the ablation rate, but deteriorates also the removal quality.

With respect to the used laser spot diameters of 24 µm and 48 µm at 515 nm and 1030 nm, respectively, it can be noticed that only 5% to 15% of the disposable laser energy has been used. This opens up the possibility of process upscaling. Regarding the determined energies per unit length, focus spot diameters of up to 280 µm at 1030 nm and 70 µm at 515 nm can be applied resulting then in up to 6 times increased ablation rates.

Conclusions

Picosecond laser removal of Al-Si layer from hot stamped steels is a promising upstream technique in the welding chain of those steels.

Laser input energies as well as the quality are strongly dependent on the laser wavelength; at 515 nm twice more energy input was required than at 1030 nm, however due to lower ablation rates the removal quality was smoother.

The achieved removal rates of up to 16 mm²/min are still insufficient for the use in an industrial environment. Hence, a process upscaling will be the challenge of future works.

Acknowledgment

The authors thank the minister for science, health and consumer protection of the free hanseatic city Bremen for the financial support.

References

1. M. Schönemann, C. Schmidt, C. Herrmann, S. Thiede, Multi-level Modeling and Simulation of Manufacturing Systems for Lightweight, Automotive Components, *Procedia CIRP 41* (2016), 1049-1054.
2. R. Heuss, N. Müller, W. van Sintern, A. Starke, A. Tschiesner, Lightweight, heavy impact. Advanced Industries, *McKinsey & Company*(2012).
3. O. Bouaziz, H. Zurob, M. Huang, Driving force and logic of development of advanced high strength steels for automotive applications, *Steel research int. 84(10)* (2013), 937-947.
4. B.A. Behrens, Hot stamping, *CIRP Ency. of Prod. Eng.*, ISBN 978-3-642-35950-7 (2014), 1-7.
5. H. Karbasian, A.E. Tekkaya,A review on hot stamping, *J. Mat. Proc. Tech. 210* (2010), 2103-2118.
6. C. Kim, M.J. Kang, Y.D. Park, Laser welding of Al-Si coated hot stamping steel, *Procedia. Eng. 10* (2011), 2226-2231.
7. H. Kügler, F. Müller, S. Goeke, F. Vollertsen, Fatigue strength of hybrid welded 22MnB5 overlap joints, *IIW Annual Assembly 2015 Com. XII*, Helsinki, Finland (2015), IIW-Doc. XII-2247-15 (online).
8. P. Norman, G. Wiklund, P. Janiak, N. Malmberg, A.F.H. Kaplan, Comparison of 22MnB5-steel with and without AlSi-coating during laser hybrid welding, *Proc. 13th Conference on Laser Materials Processing in the Nordic Countries*. (2011), 21-30.
9. M.S. Lee, J.H. Moon, C.G. Kang, Effect of the die temperature and blank thickness on the formability of a laser-welded blank of boron steel sheet with removing Al-Si coating layer, *Adv. Mech. Eng. Vol.2014* (2014), Article-ID 925493.
10. Barcellona, D. Palmeri, Effect of plastic hot deformation on the hardness and continuous cooling transformations of 22MnB5 Microalloyed Boron Steel, *D. Metall and Mat Trans A40* (2009), 1160-1174.
11. M. Windmann, A. Röttger, H. Kügler, W. Theisen, Removal of oxides and brittle coating constituents at the surface of coated hot-forming 22MnB5 steel for a laser welding process with aluminum alloys, *Surface and Coatings Technology 285* (2016), 153-160.
12. A Baladi, R.S. Mamoory, Effect of laser wavelength and ablation time on pulsed laser ablations synthesis of Al nanoparticles in Ethanol, *Inter. J. Modern Physics: Conference Series Vol. 5* (2012), 58-65.
13. Horn, M. Guillong, D. Gunther, Wavelength dependent ablation rates for metals and silicate glasses using homogenized laser beam, *Appl. Surf. Sci. 182(1)* (2001), 91-102.
14. J. Koch: Laserendbearbeitung metallischer Werkstoffe, *Werkstofftechnik Aktuell. Band 5*. Universitätsverlag Ilmenau (2011).
15. F. Bauer, A. Michalowski, T. Kiedrowski, S. Nolte,Heat accumulation in ultra-short pulsed scanning laser ablation of metals, *Optics Express 23(2)* (2015), 1035-1043.

